UDK 621.778:519.8
Review scientific article/Pregledni znanstveni članek

ISSN 1580-2949
MTAEC9, 41(1)21(2007)

THEORETICAL CALCULATION OF THE LUBRICATION-LAYER THICKNESS DURING METAL DRAWING

TEORETIČNI IZRAČUN DEBELINE PLASTI MAZIVA PRI VLEČENJU KOVIN

Dušan Ćurčija, Ilija Mamuzić

University of Zagreb, Faculty of Metallurgy, 44103 Sisak, Croatia
plutonijanac21@net.hr

Prejem rokopisa – received: 2005-09-15; sprejem za objavo – accepted for publication: 2006-10-25

The calculation of the lubricant-layer thickness using a fluid-mechanics approach is shown for the case of the cold drawing of metals. Examples of the calculation for a solid lubricant layer and a different geometry of the die entering angle are shown. The calculation of the effect of inertial force with a high drawing speed on the lubricant-layer thickness is also presented.

Key words: lubrication, Reynolds equation, mathematical modelling, Couett flowing, lubricant inertia

Predstavljen je izračun debeline plasti maziva je za vlečenje kovin na podlagi mehanike fluidov in primeri izračuna za trdno mazivo ter različno geometrijo vhoda v matrico. Predstavljen je tudi primer izračuna vpliva sile vztrajnosti na debelino mazivne plasti pri veliki hitrosti vlečenja.

Ključne besede: mazanje, Reynoldsova enačba, matematično modeliranje, Couettov tok, inercija maziva

1 INTRODUCTION

During the cold working of metals the presence of a lubricant on the surface ensures a lower extrusion force, less die wear and a reduction in the energy consumed[1]. The lubricant layer enables a greater per-pass reduction, a better surface quality and an increase in the operational stability of working devices[2,3]. It also increases the drawing speed by 50 % and the yield by 20 %[3]. In the drawing process for low and middle carbon steels, expensive industrial lubricants are substituted with soap powders[4]. The functional quality of the lubricants for drawing depends on:

- the metal drawing temperature (thermal decomposition lowers the lubricant capacity and the antifriction properties),
- the adhesive force to the covered metal surface,
- the resistance to its expulsion from the deformation area,
- the corrosion properties.

Furthermore, the lubricant should be free of compounds that have a harmful effect on human skin, an unpleasant smell or a low flash point. For metal extrusion and drawing the following lubricants are used:

- solid lubricants derived from animals, such as cattle and sheep's tallow and synthetic powders,
- liquid lubricants (machine oils and plant fats),
- emulsion oils and emulsions,
- glass lubricants[5].

For wire drawing the following lubricants are used:

- powders of calcium and sodium soaps with the addition of molybdenum disulfide powder,
- mineral oils,
- emulsions based on flour, soap and sulphuric acid,
- water dispersions of colloidal graphite.

For the drawing of tubes with a non-circular profile an iodine solution in dibutylphtalate is used as a lubricant. After working, the lubricant residue is removed by washing in hot water, and the tubes are passivated in a water solution of calcined soda and trisodiumphophate[6].

This lubricant is deposited on a phosphate base with the immersion of tubes in the solution[7] at a temperature of 70 °C to 90 °C. Also, the combined processes of the deposition of phosphate and lubricant were developed, and an improvement to the wetting angle was achieved by combining zinc phosphate and sodium soap in the water solution [8]. The immersion time was 5 min to 10 min. With longer immersion times the technological properties of the solution are impaired because of the reaction:

$$6R^0Na + Zn_3(Po_4)_2 \rightarrow 3R^0{}_2Zn + 2Na_3PO_4 \qquad (1)$$

where R^0 is the radical of the fatty acid. Also, the following reactions can occur:

$$2C_{17}H_{35}COOONa + H_2SO_4 \rightarrow \rightarrow 2C_{17}H_{35}COOH + Na_2SO_4 \qquad (2)$$

$$R^0{}_2Zn + H_2SO_4 \rightarrow 2R^0N + ZnSO_4 \qquad (3)$$

The stability of the solution is increased with the addition of a solution of caustic of soda with a pH ≈ 8. For the drawing of silver and precious-metal alloys paraffin wax and other waxes are used.

2 FLUID MECHANICS DURING LUBRICANT DRAWING

2.1 Calculation of the layer thickness for a liquid lubricant

For this calculation, Pradtl adapted the Reynolds hydrodynamic equation[9, 9/1, 9/2] and the solution

$$dp/dx = 6\,\mu v_0\,(h_0 - h)/h^3 \qquad (4)$$

is used for the calculation of the lubricant layer thickness. In the equation the inertial forces are neglected and the lubricant is treated as a Newtonian fluid[10]. Furthermore, the absence of any effect of external forces, the constant pressure over the section of the metal and the large ratio of curvature of the metals surface over the lubricant layer thickness are assumed[11]. The tool (matrix) geometry has a strong influence on the drawing process[12]. A scheme of the drawing with the lubricant corresponding to Equation (4) is shown in **Figure 1**.

The dynamic viscosity of the lubricant depends on the pressure according to the Barussa[13] law:

$$\eta = \eta_0 \exp(\gamma p)$$

For a linear change of shape in the matrix gap Ψ in **Figure 1**, the lubricant layer thickness (height) is:

$$h = h_0 - x \tan\alpha \qquad (5)$$

The change of pressure in the lubricant layer is:

$$\Delta p = -(1/\gamma)\ln[1 - 3\mu_0\,\gamma\, v_0(2 - h_0/h)/h \tan\alpha] \qquad (6)$$

For $p = p_0$ and $h = h_0$, the lubricant layer height (thickness) in the entry gap of the deformation zone is deduced as:

$$h_0 = (3\mu_0\gamma v_0)/[(1 - \exp(-\gamma p_0)] \tan\alpha] \qquad (7)$$

This solution was developed by Mizuno[1] and later confirmed by Grudev and Kolmogorov[13,14]. Also, the solution can be used:

$$h_{0v} = (9\mu_0\gamma v_0)/[4(1 - \exp(-\gamma p_v)] \tan\alpha] \qquad (8)$$

where $\quad p_v = \sigma_{t0} - \sigma_0$ and $\sigma_{t0} = 1.15\,\sigma_t \qquad (9)$

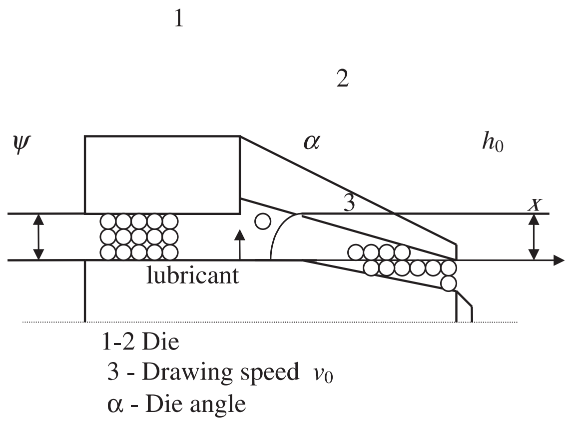

Figure 1: Scheme of die drawing with lubricant
Slika 1: Shema vlečenja z mazivom

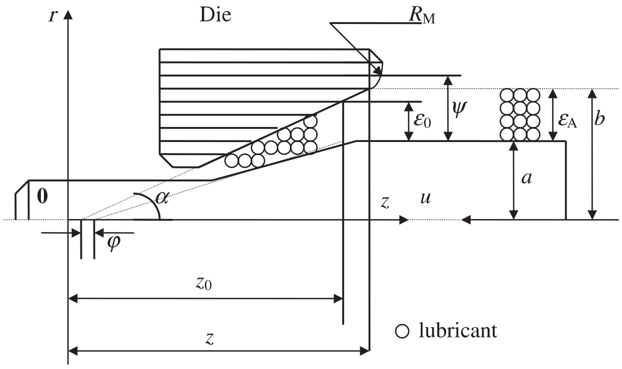

Figure 2: Modified scheme of die drawing with lubricant
Slika 2: Modificirana shema vlečenja z mazivom skozi matrico

The hydrodynamic friction was first investigated by Kameron,[15] and his findings were later confirmed by Christopherson and Naylor[15/1,15/2, 15/3].

In the modified scheme of die drawing[16] in **Figure 2** the Descartes system is shifted[17] in comparison to **Figure 1**. For the same die, the Descartes system can also be placed according to **Figure 3**[18].

For **Figure 3** the Reynolds equation written in cylindrical coordinates is:

$$1/r[\partial/\partial r(r\partial v_z/\partial r)] = (1/\mu)\,\partial p/\partial z \qquad (10)$$

$$\partial p/\partial r = 0 \qquad (11)$$

According to **Figure 2** and assuming $z = z_0$, the maximal pressure in the lubricant layer is obtained with the solution of Equation (10) for the proper boundary conditions:

$$p_{max} = -\,6\mu u\{1 - 2\varepsilon_0/(R_w - a)[1 - \varepsilon_0/2(R_w - a)]\}/ \\ /T\varepsilon_0 : R_w = \tan\alpha L_p = TL_p \qquad (12)$$

By analogy, the maximal pressure in the lubricant layer according to **Figure 3** is:

$$p_{max} = -\,(6\mu u)\,[1 - z_0/l_b]^2/(T_t - T_{op})\Delta : z_0(T_t - T_{op}) = \Delta; \\ T_t - T_{op} = \tan\alpha_1 - \tan\alpha \qquad (13)$$

The solutions according to **Figure 2 and 3** have some common factors. The lubricant's rheological

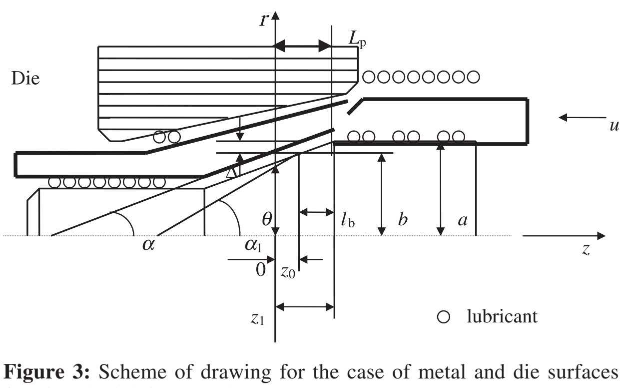

Figure 3: Scheme of drawing for the case of metal and die surfaces forming the lubricant wedge
Slika 3: Shema vlečenja za primer, ko površini kovine in matrice oblikujeta klinasti sloj maziva

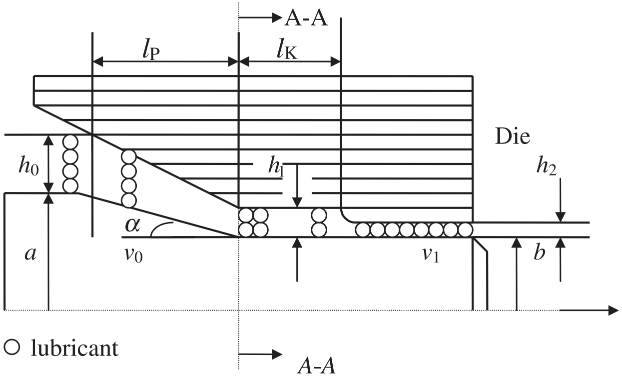

Figure 4: Drawing scheme for a complex die
Slika 4: Shema vlečenja skozi kompleksno votlico

properties are characterized by the dynamic viscosity, μ, the kinematics with the drawing speed, v, the shape of the die with the tangent (α) of the angle of the lubricant layer, T_t–T_{op}, and the thickness of the lubricant layer, ε_0 and Δ. The processing is isothermal and the effect of temperature on the lubricant viscosity can be considered to be included in the calculation of Barussa's equation.

The drawing scheme[19] for the drawing with a die of more complex design is shown in **Figure 4**.

In the Descartes system the hydrodynamic lubrication is described with the simplified Reynolds differential equation:

$$\partial p/\partial x = \mu \, \partial^2 v_x / \partial y^2 \tag{14}$$

$$\partial p/\partial y = 0 \tag{15}$$

With the boundary conditions:

$$v_x \big|_{y=0} = v_0 + \Delta v(x/l_p)^2$$

$$v_x \big|_{y=h} = h_0 - x \tan \alpha = 0 \tag{16}$$

For the simplification of the analysis the die shown in **Figure 5** is separated into two parts relative to the line A-A and the ordinate 0 – y in **Figure 5B** is the section line A –A in Figure 4A.

The pressure gradient in the lubricant layer according to **Figure 5A** is:

$$\partial p/\partial x = 6\mu \{[v_0 + \Delta v(x/l_p)^2]\,(h_0 - x\tan\alpha^*) - 2v_1 h_2\} / (h_0 - x\tan \alpha^*)^3 \tag{17}$$

By analogy, the gradient of the pressure for the scheme in Figure 5B is deduced by considering the boundary conditions:

$$v_x \big|_{y=0} = v_1$$

$$v_x \big|_{y=h1} = 0$$

$$\partial p/\partial x = 6\mu v_1 (h_1 - 2h_2)/h_1^3 \tag{18}$$

It is sufficient to know the solution of the differential equation for one side of the line A-A because both sides are related with the equation:

$$h_2 = h_1/2 + h_1^3\,[1 - \exp(-\gamma p_0)]/(12\mu_0 \gamma v_1 l_K) \tag{19}$$

The effect of inertial forces in the drawing processes is described by the equation:

$$\partial p/\partial x = 6\mu v_0/h^2 + C_1\mu/h^3 + {} + [\tan \alpha\, \rho/120h^3](16v_0^2h^2 - C_1^2) \tag{20}$$

with

$$C_1 = k/2 - [k^2/4 + 2v_0h_0(8v_0h_0 + 3k)]^{1/2} \tag{21}$$

and

$$k = 120\nu/\tan \alpha \tag{22}$$

The lubricant inertia forces[20] increase with the drawing angle and the drawing speed and decrease with a greater dynamic viscosity of the lubricant.

Besides the presented solutions of the differential equations, mathematical modelling is also applied to deduce the lubricant layer thickness[21], especially for rough surfaces[22]. The following four functions φ must be considered for the correct calculation:

$$\varepsilon/R_{as} = 7{,}72\cdot 10^{-2}\, \varphi_1(R_{apop})\, \varphi_2(R_{auz})\, \varphi_3(s_{tuz})\, \varphi_4(s_{tpop}) \tag{23}$$

where R_{as} is the average roughness, R_{apop} and R_{auz} are the longitudinal and transverse average roughness, and s_{tuz} and s_{tpop} are the roughness reference length. It is assumed that the anisotropy of the micro-relief does not affect the wear for a liquid lubricant. Empirical investigations have shown for soap powders that the ratio ε/R_{as} has values in the range 0.4 to 12.7 and 1.7 to 3.2 for the industrial oil I-8A, according to the Russian standard. These figures show that the industrial oil ensures a better regime of liquid lubrication and friction if the surface roughness is greater than the lubricant layer thickness, ε, and the orientation of the roughness affects the frictional force.

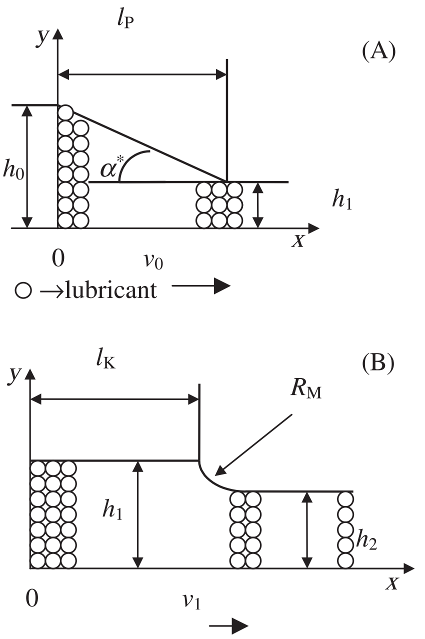

Figure 5: Two sections of **Figure 4**: a) Linear gap for lubricant flow, b) Square gap for lubricant flow
Slika 5: Dva dela **slike 4**

2.2 Calculation for a solid lubricant

According **Figure 6**, the distribution of the tangential forces[9/2] in a solid lubricant can be calculated from the solution of the equation for scheme I in **Figure 6**:

$$\tau_1 = -\tau_0 - \mathrm{d}p/\mathrm{d}x(h_2 - y) \qquad (24)$$

In the equation it is assumed that the lubricant conforms to the rheological law for a plastic substance[9/2,9/3]:

$$\tau = \tau_0 + K\,|\gamma_0|^{m-1} \cdot \gamma_0 \qquad (25)$$

The distribution of the lubricant flow speed for case II conforms to the equation[22/1]:

$$v = \frac{(h_2 - y)^{c+1}}{c+1}\left(\frac{1}{K}\frac{\mathrm{d}p}{\mathrm{d}x}\right)^{c} \qquad (26)$$

The flow of solid lubricant shown in **Figure 6** for a cold drawn tube is similar to the flow of fluid in between two parallel plates, known as Couette flow. For the calculation of the lubricant layer the thickness in the entry section of the deformation zone Kolmogorova and Ševljakova[23/1] devised the following analytical solution of Equation (26) assuming that, according to **Figure 6**, above the height h_1 the lubricant is a cooling liquid and below it is a solid lubricant:

$$\bar{K}(1-\bar{h}_1)\left[\bar{h}_2^2(3+3\bar{h}_1-2\bar{h}_2)+\bar{K}(1-\bar{h}_1)^3\right] - \qquad (27)$$
$$-2\delta\left\langle 3\bar{q}\left[\bar{h}_2^2-\bar{K}(1-\bar{h}_1)^2\right]-\bar{h}_2^3+\bar{K}(1-\bar{h}_1)^2(2+\bar{h}_1)\right\rangle = 0$$

$$2\left[2\bar{q}\bar{h}_2^2(3\bar{h}_1-\bar{h}_2)+\bar{K}\bar{h}_1(1-\bar{h}_1)^3-\bar{h}_1\bar{h}_2^3\right]\cdot$$
$$\cdot\left[\bar{K}(1-\bar{h}_{10})+\bar{h}_{10}\right]-\bar{h}_{10}\bar{h}_0\cdot\left[2\bar{K}(1-\bar{h}_{10})+\bar{h}_{10}\right]\cdot \qquad (28a)$$
$$\cdot\left[\bar{h}_2^2(3+3\bar{h}_1-2\bar{h}_2)+\bar{K}(1-\bar{h}_1)^3\right] = 0$$

$$2(1-\bar{h}_1)\left\langle\bar{q}\left[3\bar{h}_2^2+\bar{K}(1-\bar{h}_1)^2\right]-\bar{K}\bar{h}_1(1-\bar{h}_1)^2-\bar{h}_2^3\right\rangle\cdot$$
$$\cdot\left[\bar{K}(1-\bar{h}_{10})+\bar{h}_{10}\right]-\bar{h}_0\bar{K}(1-\bar{h}_{10})^2\cdot \qquad (28b)$$
$$\cdot\left[\bar{h}_2^2(3+3\bar{h}_1-2\bar{h}_2)+\bar{K}(1-\bar{h}_1)^3\right] = 0$$

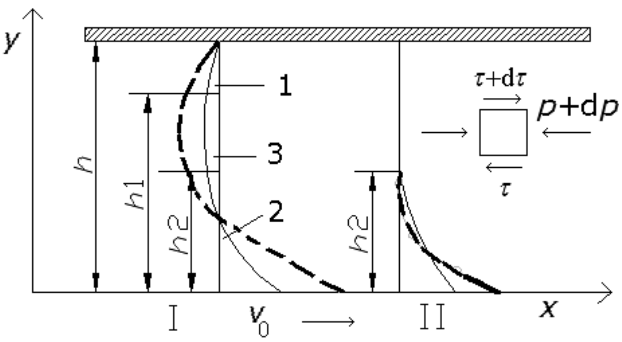

1–2, slipping flow; 3, solid layer
flow for total sticking
Flow for slipping

Figure 6: Scheme of the flowing of solid lubricant during cold drawing
Slika 6: Shema toka trdnega maziva pri hladnem vlečenju

With $\bar{q} = \dfrac{q}{v_0 h}$; $\bar{h}_1 = \dfrac{h_1}{h}$; $\bar{h}_2 = \dfrac{h_2}{h}$; $\bar{h}_0 = \dfrac{h_0}{h}$; $\bar{h}_{10} = \dfrac{h_{10}}{h}$; $\bar{K} = \dfrac{K}{\mu}$; $\delta = \dfrac{K v_0}{\tau_0 h}$

The solution for the case of the solid lubricant according to scheme[I] in **Figure 6** is:

$$\frac{2^c}{c+1}\left[h_2^{-c+1}-(1-h_1^{-})^{c+1}\right]h_{12}^{-2}-\sigma h_{12}^{-z+c}-\sigma_1(2-h_{21}^{-}-\lambda_1 h_{12}^{-})^{a_2}\cdot$$
$$\cdot(2-h_{21}^{-})h_{12}^{-a_2}+\delta_2(h_{21}^{-}-\lambda_2 h_{12}^{-})^{a_2}h_{21}^{-}h_{12}^{-a_2}=0 \qquad (28c)$$

$$\frac{2^c}{c+1}\left\langle\frac{c+1}{c+2}\left[(1-h_1^{-})^{c+2}+h_2^{-c+2}\right]+h_2^{-c+1}h_{12}^{-}\right\rangle h_{12}^{-z}+$$
$$+\sigma(q^{-}-h_1^{-})h_{12}^{-z+c}+\delta_1(2-h_{21}^{-}-\lambda_1 h_{12}^{-})^{a_1}(2-h_{21}^{-})(1-h_1^{-})h_{12}^{-a_2}+$$
$$+\delta_2(h_{21}^{-}-\lambda_2 h_{12}^{-})^{a_2}\cdot h_{21}^{-}h_1^{-}h_{12}^{-a_1}=0$$

$$q^{-}=\frac{q}{v_0 h};\ \sigma=\frac{v_0}{h}\left(\frac{K}{\tau_0}\right)^{c};\ h_1^{-}=\frac{h_1}{h};\ h_2=\frac{h_2}{h};\ \lambda_1=\frac{\tau_{s_1}}{\tau_0};$$
$$\lambda_2=\frac{\tau_{s_2}}{\tau_0};\ \delta_1=\frac{b_1 K^c \tau_0^{z-a_2}}{k^n h^{n+1}};\ \delta_2=\frac{b_2 K^c \tau_0^{z-a_2}}{k^n h^{n+1}}$$

$$h_{12}^{-}=h_1^{-}-h_2^{-};\ h_{21}^{-}=h_1^{-}+h_2^{-};\ z=1+a_1+a_2-c \qquad (28d)$$

In modern investigations of the plastic working of metals and the use of lubricants tribological principles are increasingly used[24]. Frequently, emulsions are used in combination with solid lubricants[25]. Also, the effects of decorative[26] and corrosion-protection coatings are investigated using fluid-mechanics principles. Of special practical importance is the fast development of cold drawing[27] and, as shown in this study, improvements are looked for in suitable solutions of basic fluid-mechanics equations and mathematical modelling[28] in cases when adequate solutions for the basic equations are not yet found. Polymer lubricants are being introduced because of the possibility to tailor their properties[29] and because high-speed wire drawing[30] is increasingly being used. With the development of new lubricants, special care should be given to the ecology of use and to their biological decomposition processes[31].

2.3 Examples of calculations

The drawing scheme in **Figure 2** makes it possible to model the matrix entry gap and select a determined layer thickness ε_A in the gap Ψ ahead of ε_0, the starting section of the metal deformation. In **Table 1** an example of a calculation is given for the case of the gap angle α = 0.02 rad and the value of the technological parameter:

$$A = (1 - \exp(-\gamma p_0))/6\mu\gamma v_0 = 1965512\ \mathrm{m}^{-1} \qquad (29)$$

The lubricant layer thickness in the die gap is calculated according to Equation (5).

If the geometry of the enter gap Ψ, and the geometry of the die opening according to **Figure 5B** is modelled assuming the cubic polynomial:

$$\varepsilon(x) = \varepsilon_0 - \alpha x + x^2/2R_M - \alpha x^3/2R_M^2 \qquad (30)$$

With R_M = 0.2 m, α = 0.2 rad and the technological parameter according to Equation (29) and Ψ deduced as a function of v_o, the curve in **Figure 7** is obtained. The curve series 1 is the solution of Equation (18), while the curve Poly (series 1) is obtained by using the interpolation of the polynomial (30).

Table 1: Effect of the matrix gap opening Ψ (possible entry lubricant layer thickness ε_A) on ε_0 (lubricant layer thickness at the start of the plastic deformation)
Tabela 1: Vpliv oblike odprtine matrice Ψ (možna debelina plasti maziva ε_A) na ε_0 (debelina plasti maziva na začetku plastične deformacije)

ε_A/m	ε_0/m
1.26E-05	9.98E-06
1.56E-05	1.17E-05
2.02E-05	1.41E-05
4.54E-05	2.25E-05
5.55E-05	2.45E-05
9.75E-05	2.92E-05
1.25E-04	3.07E-05
5.48E-04	3.48E-05
7.25E-03	3.54E-05
9.25E-03	3.54E-05
0.01	3.54E-05

If the lubricant is in excess ahead of the matrix gap entry section, as in **Figure 1**, there is no influence of ε_A

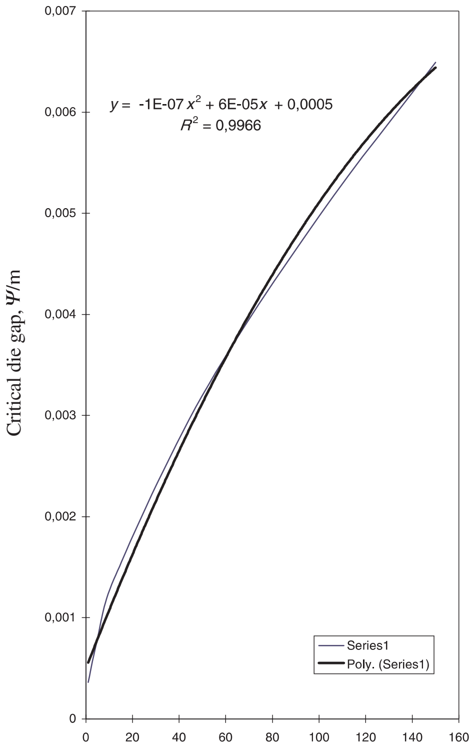

Figure 7: Effect of the drawing speed on the critical size of Ψ (section of change of ε_0 by 5 %)
Slika 7: Vpliv hitrosti vlečenja na kritično velikost Ψ (prerez, ker se ε_0 spremeni za 5 %)

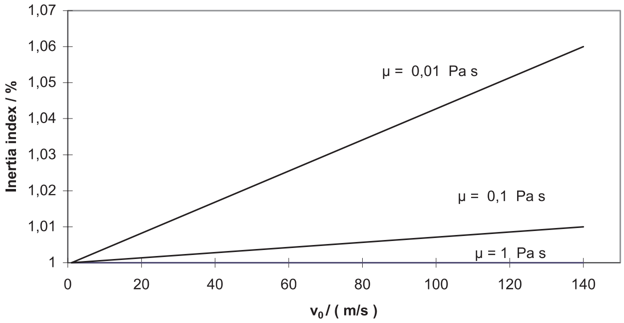

Figure 8: Effect of drawing speed on the index of inertia of the lubricant
Slika 8: Vpliv hitrosti vlečenja na indeks vztrajnosti maziva

on ε_0. However, if ε_A is lowered below 5.48E-4 m, ε_0 will also be lowered significantly. The influence of ε_A on ε_0 commences for a critical entry gap size. This is shown, for a drawing angle limited to 0.02 rad in **Figure 7**. As it is critical, the enter gap Ψ is assumed, for which the value ε_A lowers ε_0 by about 5 %. The increase of the drawing speed shifts the critical gap size to greater values of ε_A and, for this reason, the effect of drawing speed is greater for smaller drawing angles. For the correct modelling of the entering gap size of the drawing die, good results were achieved using Equation (5). For an optimal modelling radius, the effect of ε_A on ε_0 is lower. In other words, for a constant ε_A, ε_0 will be lowered more for a smaller drawing angle, while the grating of the lubricant will be greater.

In **Figure 8** the effect of the inertia index is shown for the initial section of the metal deformation zone as the solution of equations (20) and (18), with the dependence on the dynamic viscosity for a liquid lubricant and the drawing speed v_o. The index of the inertia increases with the increase of the drawing speed and the lowering of the lubricant's dynamic viscosity. For η = 1 P, the index of the inertia is negligible, as established by the previously cited authors, G. L. Kolmogorov, V. L. Kolmogorov, V. I. Meleško, V. L. Mazur and others.

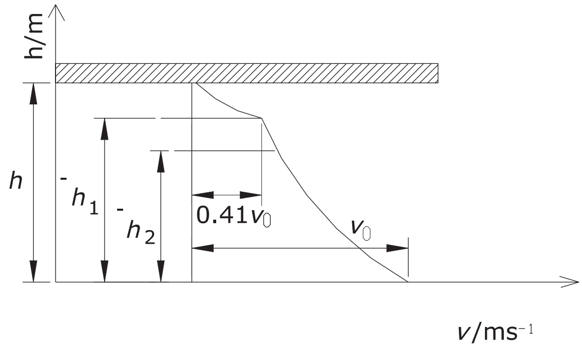

Figure 9: Calculated distribution of the speed of two liquid lubricants in the tube shaped entry die gap according to Equations (28a) and (28b) for v_0 = 16 m/s
Slika 9: Izračunana porazdelitev hitrosti po enačbah (28a) in (28b) v cevnem vhodu votlice za dve tekoči mazivi

In the case of the calculation for two emulsions with a different volume density and assuming $\bar{K} = 10$; $\delta = 2.05$; $\bar{q} = 0.5$; $\bar{h}_1 = 0.9$, the results $\bar{h}_2 = 0.7251$, $\bar{h}_0 = 0.4529$, $\bar{h}_{10} = 0.8759$ were obtained,[23] in good agreement with earlier data in ref.[I]. The lubricant speed at the level h_1 in **Figure 6** is of 0.41 v_0. The results of these calculations are in good agreement with calculations based on Equations (28a) and (28b) given in several references for the case of two liquid lubricants of different specific density separated at the height $\bar{h}_1$, as shown approximately in **Figure 9**.

In **Table 2** the results of the calculation for a fat lubricant are shown as a solution of the Equations (28c) and (28d) for the conditions equal to those in[23/1,23/2]: $\sigma_1 = 0$; $\sigma_2 = 0$; $m = 1$; $c = 1$; $z = 2$; $a_1 = a_2 = 0$.

Table 2: Calculations for a fat lubricant and total lubricant sticking
Tabela 2: Izračun na trdno mazivo (mast) in popolno oprijetost maziva

δ	$h_1^- - h_2^-$
7	0.686296 – 0.641544 = 0.044752
6	0.68923 – 0.637575 = 0.0516
5	0.693 – 0.632 = 0.061
4.5	0.696097 – 0.628717 = 0.06734
4	0.699336 – 0.624449 = 0.0748
3	0.708732 – 0.612105 = 0.0966
2.5	0.71572 – 0.60273 = 0.11299
2	0.72556 – 0.589477 = 0.1361

According to these results, the thickness of the solid lubricant layer 3 in **Figure 6** decreases with the increase of δ.

3 CONCLUSION

In the article a short survey of the theory of the application of lubricants for the cold-drawing processes of metals is given. The dies are presented in different coordinate systems with the aim of more easily finding the analytical solutions for the basic fluid mechanics differential equations necessary for the calculation of the lubricant-layer thickness. The solutions of the basic equations are shown for liquid and solid lubricants, and the combination of both, and the calculation of the change of lubricant layer thickness in the section of the deformation zone in the entry section of the working die.

For the case of the laminar flow of non-compressible lubricants, the analytical solutions of Reynolds differential equations give acceptable results. For the case of insufficiently lubricated surfaces with a greater roughness and hydrodynamic lubrication, it is not yet possible to use analytical solutions of Reynolds equations, and for this reason, mathematical modelling is used[32]. Also, the effect of lubricant inertia forces is considered for high drawing speeds used to increase the angle significantly [33].

Symbols not explained in the text

Symbol	Unity	Significance
A	m^{-1}	Technological parameter
pH	number	Negative log of the concentration of hydrogen ions
R^0	–	Radical of fat acids
R_w, R_M	m	Parameter of the deformation zone and die radius
p, p_0	Pa	Pressure in the lubricant layer and in the entering section of the deformation zone
x, y, z, r	m	Descartes coordinates and cylindrical coordinates
μ, μ_0	Pa s	Lubricant dynamic viscosity for the pressures p and p_0
v_0, v_z	m/s	Metal drawing speed with movement along the longitudinal axis z
h_0, h	m	Lubricant thickness on the entering section of the deformation zone and in the die gap
γ	m^2/N	Piezo-coefficient of the lubricant viscosity
exp, tan	2.718...	Basis of the natural log and tangent of the metal-drawing die
h_{ov}	m	Lubricant layer thickness determined using the variation calculation
σ_{t0}, σ_0	N/m^2	Metal yield stress and tensile strength
ν	m^2/s	Kinematic viscosity
q	m^2/s	Lubricant volume consumption per length of the drawn metal
ρ	kg/m^3	Fluid density
ε_A	m	Lubricant layer thickness ahead of the die entry gap
α, α^*	rad	Drawing angle (α^* is the rotated angle related to α)
Ψ	m	Die gap that can be filled with lubricant (difference between the diameter of the die opening and the sum of the rod + the lubricant thickness
a	m	Initial tube size
b	m	$b = a + \varepsilon_A$
v_z, u	m/s	Speed along the longitudinal axis z and the metal drawing speed
z_0	m	Distance of the lubricant layer with the thickness Δ from the initial point
l_p, l_K	m	Design characteristics of the die in the deformation zone
τ	Pa	Tangential stress
τ_0, K, m		Grease rheological constants
γ_0		Gliding speed
Δ	m	Lubricant layer thickness in **Figure 3**
θ	m	Ordinate of rupture of the lubricant wedge

Translation from Croatian: prof. dr. Franc Vodopivec

4 REFERENCES

[1] Pešić M., Milenković V., Hladno izvlačenje žica, šipki i cevi, Tehnička knjiga, Beograd 1965, 191–192
[2] Molčanov M. M, Nosov V. A., Romanec V. A., Metallurg 26 (**1981**) 7, 38–40

[3] Čekmarev A. P., Meleško V. I., Mazur V. L., Stalj 39 (**1969**) 12, 1108–1111
[4] Tračak S. V., Kačur V. I., Hohlova M. P., Stalj 49 (**1979**) 10, 789–791
[5] Mamuzić I., Drujan V. M., Teorija materijali tehnologija čeličnih cijevi, Hrvatsko metalurško društvo, Zagreb, 1996, 214
[6] Jakovliev V. V., Semeljnickij B. L., Baljavin V. A., Stalj 42 (**1972**) 6, 82
[7] Štanko V. M., Novikov V. G., Lipkin Ja. N., Stalj 41 (**1971**) 10, 933
[8] Grebenšćikova A. Z., Stalj 29 (**1959**) 10, 932
[9] Ivušić V., Tribologija, HMDT ISBN 96038-3-8, Zagreb 1998
Kolmogorov G. L., Gidrodinamičeskaja smazka pri obrabotke metallov davlenniem, Moskva, Metallurgija 1986, 168
Kolmogorov V. L., Orlov V. L., Kolmogorov G. L., Gidrodinamičeskaja podača smazki, Moskva, Metallurgija 1975, 256
[10] Zikov Ju. S., Izvestija Černaja metallurgija 30 (**1987**) 4, 52–53
[11] Zikov Ju. S., Teorija prokati, teoretičeskie problemi prokatnogo proizvodstva, Metallurgija, Moskva 1975
[12] Iharoš B., Metalurgija 11 (**1972**) 3–4, 3
Iharoš B., Metalurgija 12 (**1973**) 1, 31
Iharoš B., Metalurgija 12 (**1973**) 2, 21
[13] Kolmogorov G. L., Izveszija Černaja metallurgija 26 (**1983**) 10, 68
[14] Mizuno T., Japon J. Soc. Techn. Plast 7 (**1966**) 6, 383–389
[15] Christopherson D. G., Naylor H., Wire Ind., 22 (**1955**) 7, 260
Christopheron D. G., Naylor H., Proc. Inst. Mech. Engrs., (**1955**) 8, 169
Christopheron D. G., Naylor H., Wire Production 4 (**1955**) 5
[16] Nedovizij I. N., Trudi konferenci po metiznomu proizvodstve 15–21 marta 1959. CBTI Čeljabinskogo sovnarhoza
[17] Perlin I. L., Šapiro V. Ja., Školjnikov E. L., Izvestija Cvetnaja metallurgija 6 (**1963**) 5, 130–137
[18] Kolmogorov V. L., Sb., Inžinernie metodi rasčeta tehnologičeskih procesov obrabotki metallov davleniem, Metallurgizdat, Sverdlovsk, 1961
[19] Kolmogorov G. L., Izvestija Černaja metallurgija 16 (**1973**) 8, 76
[20] Kolmogorov G. L., Sjanov S. P., Izvestija Černaja metallurgija 30 (**1987**) 10, 35
[21] Jurković M., Hriešik A., Jurković Z., Vitez I., Metalurgija 37 (**1988**) 3, 159–163
[22] Grudev A. P., Dolžanskij A. M., Sigalov B. Ju., Kovalev V. S., Izvestija Černaja metallurgija 31 (**1988**) 2, 52–54
[23] Ševljakov V. Ju., Kolmogorov G. L., Izvsetija Černaja metallurgija 31 (**1988**) 10, 67–70
Ševljakov V. Ju., Prevadčuk V. P., Izvestija Černaja metallurgija 31 (**1988**) 5, 61–65
Prevadčuk V. P., Ševljakov V. Ju., Izvestija Černaja metallurgija 27 (**1984**) 11, 74–77
[24] Kolmogorov V. L., Fedotov A. V., J. Mater. Process. Technol., 95 (**1999**) 1–3, 55–64
Kuznetsov S. A., Vinogradov S. I., Semenov S. Y., Graber E. A., Proizvod. Prokata July (**1999**) 7, 26–28
[25] Belosevich V. K., Ionov S. M., Proizvod. Prokata August (1999) 8, 3–6
[26] Mamuzić I., Drujan V. M., Teorija materijali tehnologija čeličnih cijevi, Hrvatsko metalurško društvo, Zagreb 1996, 444
Sukurai M., Hiraya A., Hashimoto S., Techn. Rev., 80 (**1999**), 71–77
[27] Zaccone D. C., Bodnar J. J., Elko R. G., Grivna J. M., J. M. Trans. J. Mater. Manuf., 107 (**1998**), 26–24
Me D. M., Liu S. P., Zheng J. F., Met. Form. Technol. 20 (**2002**) 5, 29–32
Bao P., Cheu X. P., Jiany N. M., Met. Form. Technol. 20 (**2002**) 2, 8–10
Keun Y. T., Lee B. H., Wagoner R. H., J. Mater. Process. Technol. 130 (**2002**), 60–63
[28] Liu Y. J., Tieu A. K., J. Mater. Process. Technol. 130 (**2002**), 202–207
Kim B. M., Kim D. H., Jeong D. J., Key Eng. Mater., (**2003**), 233–236, (Part I) 377–382
[29] Blanchourd C. R., Crowinshield R. D., Johanson T. S., Laurent M. P., Wear, 255 (**2003**) 1, 780–784
[30] Artemov V. V., Demyanova V. I., Frolov V. I., Grunko B. N., Stal 73 (**2003**) 5, 59–63
[31] Kržan B., Vižintin J., Biorazgradivo mazivo za duboko izvlačenje na osnovu biljnih ulja, XXXVI Stručno-znanstveni simpozij, Maziva 2003, Rovinj, Croatia, 22–24. 10. 2003
[32] Kolmogorov V. L., Computers and Structures, 44 (**1992**) 1–2, 419–424
[33] Ćurčija D., Mamuzić I., Metalurgija 44 (**2005**) 2, 113–117